Environment Canada Environnement Canada

Canada

Interannual and seasonal variability of the surface energy balance and temperature of central Great Slave Lake

W.R. Rouse, C.M. Oswald, J. Binyamin, P.D. Blanken, W.M. Schertzer and C. Spence

NWRI Contribution 02-022

Interannual and Seasonal Variability of the Surface Energy Balance and Temperature of Central Great Slave Lake

WAYNE R. ROUSE, CLAIRE M. OSWALD, AND JACQUELINE BINYAMIN

School of Geography and Geology, McMaster University, Hamilton, Ontario, Canada

PETER D. BLANKEN

Department of Geography, University of Colorado, Boulder, Colorado

WILLIAM M. SCHERTZER

National Water Research Institute, Burlington, Ontario, Canada

CHRISTOPHER SPENCE

Environment Canada, Yellowknife, Northwest Territories, Canada

(Manuscript received 26 September 2002, in final form 5 February 2003)

ABSTRACT

This paper addresses interannual and seasonal variability in the thermal regime and surface energy fluxes in central Great Slave Lake during three contiguous open-water periods, two of which overlap the Canadian Global Energy and Water Cycle Experiment (GEWEX) Enhanced Study (CAGES) water year. The specific objectives are to compare the air temperature regime in the midlake to coastal zones, detail patterns of air and water temperatures and atmospheric stability in the central lake, assess the role of the radiation balance in driving the sensible and latent heat fluxes on a daily and seasonal basis, quantify magnitudes and rates of the sensible and latent heat fluxes and evaporation, and present a comprehensive picture of the seasonal and interannual thermal and energy regimes, their variability, and their most important controls. Atmospheric and lake thermal regimes are closely linked. Temperature differences between midlake and the northern shore follow a seasonal linear change from 6°C colder midlake in June, to 6°C warmer in November–December. These differences are a response to the surface energy budget of the lake. The surface radiation balance, and sensible and latent heat fluxes are not related on a day-to-day basis. Rather, from final lake ice melt in mid-June through to mid- to late August, the surface waters strongly absorb solar radiation. A stable atmosphere dominates this period, the latent heat flux is small and directed upward, and the sensible heat flux is small and directed downward into the lake. During this period, the net solar radiation is largely used in heating the lake. From mid- to late August to freeze up in December to early January, the absorbed solar radiation is small, the atmosphere over the lake becomes increasingly unstable, and the sensible and latent heat fluxes are directed into the atmosphere and grow in magnitude into the winter season. Comparing the period of stable atmospheric conditions with the period of unstable conditions, net radiation is 6 times larger during the period of stable atmosphere and the combined latent and sensible heat fluxes are 9 times larger during the unstable period. From 85% to 90% of total evaporation occurs after mid-August, and evaporation rates increase continuously as the season progresses. This rate of increase varies from year to year. The time of final ice melt exerts the largest single control on the seasonal thermal and energy regimes of this large northern lake.

1. Introduction

This research on Great Slave Lake is part of the Canadian Global Energy and Water Cycle Experiment (GEWEX) Enhanced Study (CAGES), an undertaking within the Mackenzie GEWEX Study, initiated in order to better understand and model energy and water cycles in the Mackenzie River basin (MRB), and to assess changes to these cycles that may arise from natural climate variability and anthropogenic climate change (Stewart et al. 1998; Rouse et al. 2003).

Great Slave Lake (GSL) (Fig. 1) is the fifth largest lake in North America in terms of surface area (28 568 km^2), and the mean depth of the main lake, exclusive of the eastern arm, is estimated from bathymetric anal-

Corresponding author address: Wayne R. Rouse, School of Geography and Geology, McMaster University BSB 311, Hamilton, ON L8S 4K1, Canada.
E-mail: rouse@mcmaster.ca

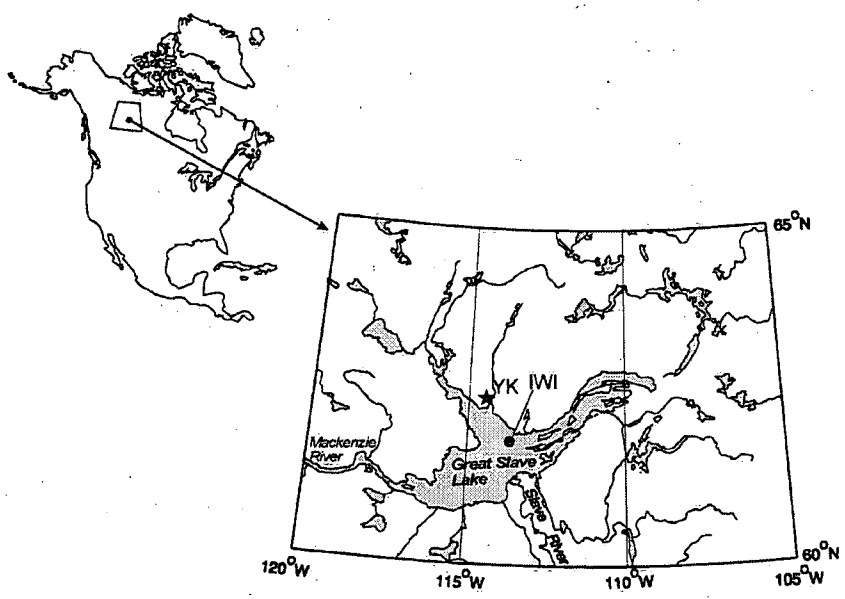

FIG. 1. Location of the main research site on the largest of the Inner Whaleback Islands, Great Slave Lake; YK and IWI are shown.

ysis at 32 m (Schertzer et al. 2000a). It is one of four very large lakes in the MRB, the others being Great Bear Lake, which is slightly larger, and the Lake Athabasca and Lesser Slave Lake, which are both substantially smaller. The combined area of the lakes at 69 000 km^2 represents 3.8% of the total area of the MRB.

The study focuses on GSL as a representative of very large lakes in the Mackenzie basin and addresses interannual variability in the thermal regime and surface energy fluxes midlake during a 3-yr open-water period. Two of these years overlap the CAGES water year and the third takes place in the year prior to CAGES. The specific objectives of this research are to 1) compare the air temperature regime in central GSL to the northern coast at the city of Yellowknife (YK), Northwest Territories, Canada, 2) examine seasonal and interannual patterns of air and water temperatures and atmospheric stability in the central lake, 3) document the radiation balance and assess its role in the sensible and latent heat fluxes on a daily and seasonal basis, 4) assess magnitudes and rates of the sensible and latent heat fluxes and evaporation, and 5) develop a comprehensive picture of the seasonal and interannual thermal and energy regimes and their variability.

Relevant research on GSL has been reported in Blanken et al. (2000), Rawson (1950), Rouse et al. (1999, 2000, 2002), and Schertzer et al. (1999, 2000a); and related research on the Laurentian Great Lakes, to which GSL bears many similarities, is presented by Schertzer (1997). General information resulting from these studies is summarized as follows. Large temperate and high-latitude lakes act as major reservoirs of energy due to their large heat capacities. After final ice melt most of the solar radiation goes into warming these lakes, and little is available for evaporation or sensible heating of the atmosphere. Lake heat content peaks in late summer and early fall, after which time release of the stored energy commences. In late fall and early winter, when solar radiation is small, this energy is released as latent and sensible heat fluxes to the atmosphere. Thus, large lakes introduce a large seasonal thermal lag into the landscape. The release of latent and sensible heat on a day-to-day basis is driven primarily by the wind. Strong winds and thermal convection mix the upper water of the lake, bringing stored heat to the surface, after which strong mechanical turbulence and/or free convection moves it upward into the atmosphere. Lake waters are warmest near the shore in early summer and in central-lake areas in early winter. Generally winds are largest midlake where the fetch is maximum. These factors interact to influence spatial variations in the magnitudes of the sensible and latent fluxes.

Many of the above findings will be reinforced in results of this 3-yr study in central GSL, and evidence indicating significant temporal variability will be introduced.

2. Site and methods

a. Site

The research was carried out from the largest of the Inner Whaleback Islands (IWI) (61.92°N, 113.73°W), a group of small rock islands located in the main body of Great Slave Lake, 80 km southwest of Yellowknife (Fig. 1). The nearby waters average a depth of 50 m that is characteristic of the central part of the lake. The wind fetch exceeds 12 km in all directions, and the

island's height (above mean water level), width, and length are approximately 10, 100, and 180 m, respectively (Blanken et al. 2000). Temperature comparisons are made with the airport weather station at Yellowknife. For such comparisons the measurements are standardized to meteorological screen height.

b. Radiation balance

Component fluxes of the radiation balance are described as

$$Q^* = \mathrm{K}\downarrow - \mathrm{K}\uparrow + \mathrm{L}\downarrow - \mathrm{L}\uparrow, \quad (1)$$

in which Q^* is net all-wave radiation, K↓ is incident solar radiation, K↑ is reflected solar radiation, L↓ is incoming longwave sky radiation, and L↑ is outgoing longwave radiation from the lake surface.

Details of the instrumental setup in 1997 and 1998 are given in detail in Blanken et al. (2000) and will only be described briefly here. In 1997 a 14-m-long retractable horizontal boom, positioned 2-m above the mean water surface, was constructed on the eastern side of the island; Q^* was measured with a net radiometer (Kipp and Zonen, model NR Life) mounted on the end of the boom. Calculations indicated that 95% of the instrument's signal received from the water surface originated from a circle with a radius of 8.7 m. With an average water depth of 9 m, radiation measurements were considered free of the island's influence (Blanken et al. 2000). Water surface temperature, Tw_0, was measured with an infrared thermometer (Everest Interscience, model 4000.GL) also mounted at the end of the boom, with a viewing angle of 45° and a viewing cone of 15°; L↑ was determined as $\mathrm{L}\uparrow = \varepsilon\sigma T w_0^4$ in which ε is surface emissivity (0.97 for water), and σ is the Stefan–Boltzmann constant. Upward- and downward-facing pyranometers (Eppley Laboratories) measured K↓ and K↑, the latter mounted at the end of the boom. All instruments were calibrated prior to field installation. Signals were sampled at 2-s intervals and stored as 10-min means in a datalogger (Campbell Scientific, model CR10X). The 12-V batteries that were charged by a solar panel supplied power. And L↓ in Eq. (1) was derived as a residual.

The boom and its instruments were destroyed in 1998 by late winter ice thrusting and were replaced with a near-identical setup. The replacement boom and sensors were again destroyed, this time by high storm waves in 1998. In the spring of 1999, a different tack was taken. The equipment was removed to the steep south edge of the island. In Eq. (1) Q^* was obtained from the component fluxes.

The IR thermometer (giving L↑) was focused at an angle that took in a large swath of unobstructed water (average depth about 50 m) to the south, but did not include the horizon or sky. The value for surface albedo, derived through the previous two field seasons (Blanken et al. 2000), was utilized rather than K↑, which was not measured. A pyranometer was used to determine K↓, and L↓ was measured using a pyrgeometer (Eppley Laboratories). All radiation instruments were routinely calibrated or recalibrated prior to field installation in each of the years of measurement.

c. Energy balance

The one-dimensional energy balance for the lake is given by

$$Q^* = Q_E + Q_H + Q_{\mathrm{ST}}, \quad (2)$$

in which Q_E, Q_H, and Q_{ST} are the latent and sensible heat fluxes and change in stored heat energy in the lake, respectively, Q_E and Q_H are positive when directed from the surface into the atmosphere, and Q_{ST} is positive when the lake is gaining heat. Measured directly as eddy covariances, Q_E and Q_H (Blanken et al. 2000) give

$$Q_E = L_v w'\Delta_v', \quad (3)$$

$$Q_H = C_a w'\mathrm{T}', \quad (4)$$

where L_v and C_a are the latent heat for vaporization of water vapor and heat capacity of air, respectively, and $w'\Delta_v'$ and $w'\mathrm{T}'$ are the eddy covariances of vertical wind and water vapor concentration, and vertical wind and air temperature, respectively. The equivalent millimeter of evaporated water, E is given by Q_E/L_v. A Hydra eddy covariance system (United Kingdom Hydrological Institute, Hydra MK2) was employed for the eddy covariance measurements. The Hydra's characteristics have been described in detail by Shuttleworth et al. (1988) and Blanken et al. (2000). It was mounted 7 m above the ground and ran successfully throughout the three field seasons. Its accuracy, response times, and running characteristics were carefully checked prior to each measurement period. As detailed by Blanken et al. (2000), 80% of the measured eddy fluxes were obtained from within upwind horizontal distances of 4.9, 5.9, and 8.4 km, for daytime, neutral, and nighttime periods, respectively. This lay well within the fetch distance of 12 km to the nearest land. The rate of change of heat storage in the lake in Eq. (2), Q_{ST}, applies to a one-dimensional water column at Inner Whaleback Islands, and is derived as a residual. This residual compares favorably to Q_{ST} calculated calorimetrically for the whole lake by Schertzer et al. (2003).

Additional instruments were positioned 8.5 m above the ground (18 m above the water surface) on a Meteorological Service of Canada (MSC) tower near the center of the island. Wind speed, u_{18}, and direction (R. M. Young, model 5310), and relative humidity (used to calculate vapor pressure, e_{18}) and air temperature (Ta_{18}) (Gill Instruments, model HMP-35D) were all measured from this tower and were recorded in a datalogger (Campbell Scientific, model 21X) as 10-min means based on 2-s sampling times. These data were reduced to normal screen measurement height above the lake,

TABLE 1. Periods of instrumental measurements at Inner Whaleback Island. The bracketed number gives total days of measurement as a percent of open-water days.

Period	Radiation balance	Sensible and latent heat fluxes	Water temperature	Open-water days
1997	25 Jul–9 Sep (26%)	26 Jul–10 Sep (27%)	1 Aug–10 Sep (23%)	176
1998	27 Jun–6 Aug (19%)	24 Jun–25 Sep (44%)	20 Jun–12 Sep (41%)	212
1999	12 Jun–15 Dec (102%)	12 Jun–18 Nov (89%)	17 Jun–29 Sep (57%)	184

using log-linear relationships, and were used for periods when eddy correlation measurements were not made (usually early and late in the open-water season), for determining E from mass transfer calculations of the type

$$E = -K_z u_z \Delta e, \quad (5)$$

in which K_z is a diffusion coefficient for height z above the water surface, u_z is horizontal wind speed at height z, and Δe is the difference between atmospheric vapor pressure at height z and saturation vapor pressure at water surface temperature T_{w0}. As outlined in detail in Blanken et al. (2000), K_z is determined empirically using measured vapor fluxes. Such determinations have been used widely and successfully in calculating evaporation from lakes, small and large (e.g., Harbeck 1962; Quinn 1978; Quinn and den Hartog 1981).

d. Water temperatures

A water temperature profile was measured 1 km southwest of the island in 60 m of water. Water temperatures, T_w, at depths of 0.7, 5, 10, 15, 20, 25, 35, and 55 m were measured with a thermistor and a datalogger, each encapsulated in a watertight container (Onset Computer Corp., model TidbiT). Their accuracy was calculated at 0.23°C, spanning a 0°–23°C temperature range (Blanken et al. 2000). Temperatures were sampled simultaneously every 15 min. The same storm that destroyed the boom in August 1998 also destroyed the water temperature profile, and all of the 1998 data were lost. Fortunately, measurements from a nearby set of thermistors at similar depths were available and, in 1999, a replacement buoy and thermister string at IWI (see, Schertzer et al. 2002) operated successfully throughout much of the ice-free period. Surface water temperatures (as shown in Fig. 3) combine observations from the Inner Whaleback Islands and the top level of the thermistor string. On a daily average basis, the surface waters in central GSL are mixed sufficiently so that thermistor measurements at 0.7 m and at the surface are within 0.3°C of one another.

TABLE 2. Dates of FT, FF, air temperature differences (°C) between Inner Whaleback Island and Yellowknife A ($\Delta T_a = T_{a\mathrm{IWI}} - T_{a\mathrm{YK}}$) at FT and FF ($\Delta T_a$FT and ΔT_aFF), and the date on which temperatures at Inner Whaleback and Yellowknife are the same ($\Delta T_a = 0$).

Year	FT	FF	ΔT_aFT	ΔT_aFF	$\Delta T_a = 0$
1997	21 Jun	14 Dec	−2.8	2.3	12 Sep
1998	3 Jun	1 Jan (1999)	−6.0	7.5	30 Aug
1999	11 Jun	12 Dec	−6.1	6.6	6 Sep
Avg	12 Jun	19 Dec	−5.0	5.5	6 Sep

e. Measurement periods

Periods of measurement of the various fluxes and parameters were variable during the 3 yr with respect to dates and the percentage of the open-water days represented (Table 1). Open-water days are accumulated from the period in spring when there is no longer any shorefast ice, but there may still be patches of drifting ice, through to the establishment of a permanent ice cover the following winter. They have been determined from analysis of passive microwave images to determine dates of final spring thaw and final freeze up (Table 2) provided by A. Walker (2001, personal communication), using methodology described in Walker et al. (1999). The percentage of the open-water period that included measurement days for the various parameters varied from 19% in 1997 up to all of the open-water period in 1999 (Table 1).

3. Results

a. Air temperature

The nearest land-based meteorological station to IWI is at the city of YK a straight-line distance of 80 km from IWI. Table 3 indicates that at YK, the three study years were all substantially warmer than the long-term average for the 7 months spanning the open-water season on GSL. The very pronounced El Niño warming in the late 1990s is especially evident in early winter of 1997 and throughout 1998. Only 2 of the 21 months of the study periods were colder than average.

The temperature differences between IWI and YK during the open-water season can be pronounced (Fig. 2). On average, for the 3 yr, these differences, $\Delta T_a = T_a\mathrm{IWI} - T_a\mathrm{YK}$, are accurately described by a linear trend line (Fig. 2) that yields a coefficient of determination $r^2 = 0.80$. Table 2 indicates that on 12 June the average date of final thaw (FT) of GSL, $\Delta T_a = -5.0$, and on 19 December the average date of final freeze (FF), $\Delta T_a = 5.5$. The date of temperature equilibration between the two sites, $\Delta T_a = 0$, occurred on 6 September. Annual differences in the 3 yr are evident in the open-water period. In 1998 FT occurred 1 week earlier than in 1999, and almost 3 weeks earlier than in 1997. In 1998 FF occurred almost 3 weeks later than in 1997

TABLE 3. Monthly mean temperatures (T_m) at Yellowknife airport (°C) for the study periods compared to the 30-yr long-term average (LTA) and departures from the long-term average (T_m − LTA).

Year	Jun	Jul	Aug	Sep	Oct	Nov	Dec	Avg
1997	13.4	17.8	15.7	9.8	−4.4	−9.6	−15.9	3.9
1998	15.4	19.1	15.9	8.6	2.4	−6.8	−19.1	5.1
1999	13.4	15.1	15.2	7.7	−1.1	−9.2	−20.3	3.0
LTA	12.9	16.3	14.1	6.7	−1.6	−14.1	−24.0	1.5
				T_m − LTA				
1997	0.5	1.5	1.6	3.1	−2.8	4.5	8.1	2.4
1998	2.5	2.8	1.8	1.9	4.0	7.3	4.9	3.6
1999	0.5	−1.2	1.1	1.0	0.5	4.9	3.7	1.5

and 1999 (Table 2). The open-water period was 15% and 20% longer in 1998 than in 1999 and 1997, respectively.

b. *Water temperature*

Daily mean surface water temperature, T_{w0}, reached 20°C on several occasions in 1998 during the measurement periods (Fig. 3). The polynomial fits to T_{w0} (Fig. 3) generally agree with the interannual variability in final thaw in 1998 and 1999 (Table 2), the years with enough data to allow a seasonal curve fit. However, subfreezing water temperatures were measured well prior to the dates of final freeze shown in Table 2, notably in 1999 (Fig. 3). There appears to be a substantial time lag between the freezing of the water surface and the release of enough heat to allow final hard freeze of the water column. The central CAGES year of 1998 is noteworthy for the very warm surface temperatures in early summer and throughout the fall and early winter (Fig. 3).

Large interannual differences in lake temperatures in the top 10 m are evident in Fig. 4 with much higher temperatures in 1998 than in 1999. The differences persisted from early in the open-water period to middle August when all temperatures in this layer converged. The thermal regime in this layer can change rapidly over time as large wind events exert strong mixing (Blanken et al. 2000; Schertzer et al. 2000a). In contrast, the 10–50-m layer shows a gradual and linear seasonal temperature increase, and there is little difference between the 2 yr.

c. *Air and water temperatures and atmospheric stability*

Figure 5 indicates that average daily IWI air temperatures (T_aIWI) are much greater than average daily surface water temperatures (T_{w0}), following final ice melt in June, and remain higher until temperatures equilibrate in August. In the subsequent interval through to freeze up, $T_{w0} > T_a$IWI. The trend lines in Fig. 5 indicate that equilibration occurs about 9 August in 1998 and 22 August in 1999. Thus, atmospheric thermal stability generally persists throughout much of the summer season, engendering the stable regime turbulent transfer processes documented by Blanken et al. (2003). Assuming that a stable lower atmosphere persists from final thaw (Table 2) to $T_a = T_{w0}$ (Fig. 5), and that an unstable atmosphere persists from $T_a = T_{w0}$ to final freeze, one

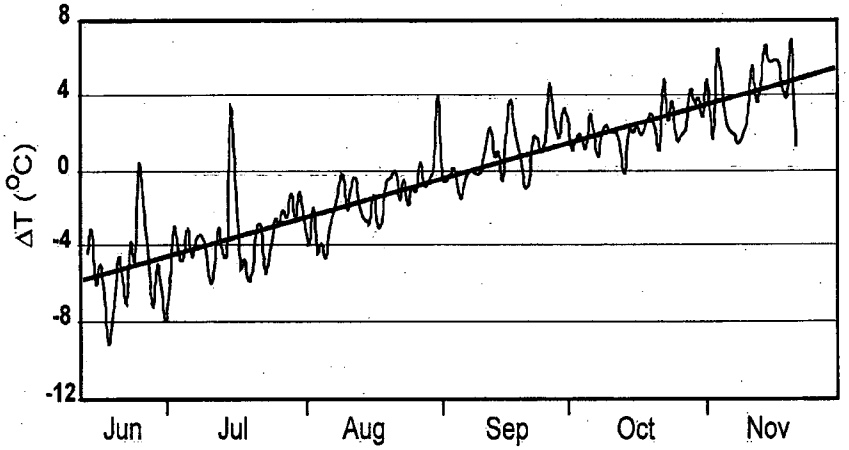

FIG. 2. Temperature differences (°C) between central Great Slave Lake at Inner IWI and YK airport averaged for the 3 yr of measurement during the open-water season.

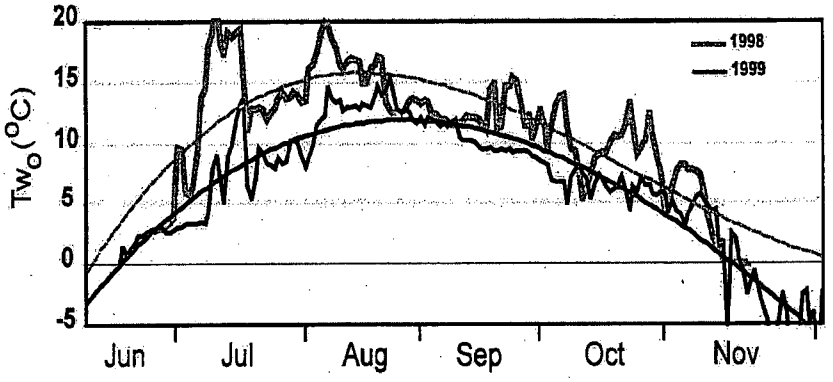

FIG. 3. Water surface temperatures (T_{w0}) on Great Slave Lake for 1998 and 1999 with third-order polynomial line fits to the data.

can calculate the approximate length of the period of stable and unstable lower atmospheric conditions during the open-water season. In 1998 this gives 67 and 145 days, respectively, whereas in 1999, the corresponding periods are 72 and 112 days. Thus, in 1998 the period when sensible and latent fluxes are likely to be directed downward to the lake surface is 7% shorter than in 1999, and the period when sensible and latent heat fluxes are likely to be directed upward from the lake surface is 30% longer.

d. Radiation balance

The fully open-water season begins in June and persists into December (Table 2) and, thus, is primarily concentrated between the summer and winter solstices. This is evident in Fig. 6, which shows the extraterrestrial radiation, K_0, decreasing from a maximum of 474 to a minimum of 25 W m^{-2}. In summer [June–July–August (JJA)], as is common with its temperate counterparts, Great Slave Lake is a high-energy system. Absorbed solar radiation, $K^* = K\downarrow - K\uparrow$, has a magnitude that equals 52% of K_0, and Q^* has a magnitude equal to 40% of K_0. In midsummer, during a common period for the 3 yr when all instruments were operating, differences in the radiation balance are small (Table 4). As K^* gets very small in November and December, Q^* converges on the net longwave radiation, $L^* = L\downarrow - L\uparrow$, until they become equal during the high-latitude polar night (Fig. 6). In the open water season L^* tends to be large, as seen in Table 4 and Fig. 6. The outgoing component, $L\uparrow$, varies only slowly over time (Fig. 7) due to the conservative lake surface temperature regime, whereas the incoming component, $L\downarrow$, is much more variable, being influenced by changing atmospheric temperature, humidity, and cloud conditions. Thus, the large variability in L^* seen in Fig. 6 is primarily due to the fluctuations in $L\downarrow$.

e. Sensible and latent fluxes

On a daily and a seasonal basis the surface sensible and latent heat fluxes are not strongly influenced by the net radiation (Fig. 8); Q^* decreases from its high values at the summer solstice to negative values in November, whereas the sensible and latent heat fluxes, Q_H and Q_E,

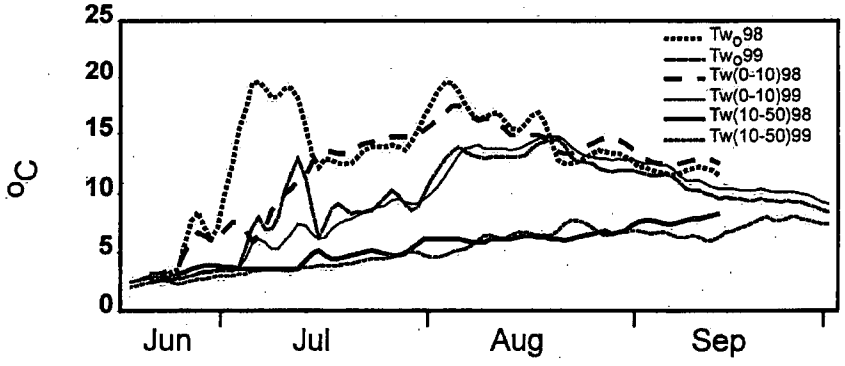

FIG. 4. Three-day moving averages of water temperatures at various depths, as measured from buoy strings near Inner Whaleback Island; T_{w0} is surface temperature, T_w (0–10) represents the top 10 m of water and T_w (10–50) is the interval from 10 to 50 m, and 98 and 99 are the designations for 1998 and 1999, respectively.

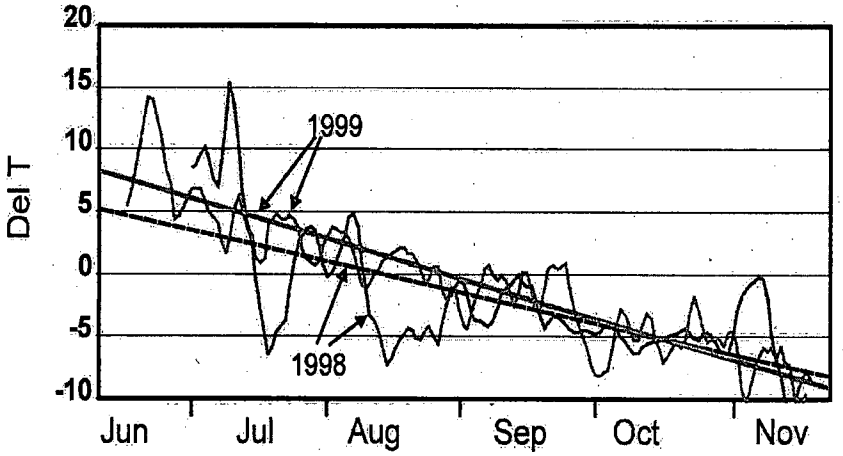

FIG. 5. Seasonal temperature differences between air and lake surface (Del $T = T_a - T_{w0}$) for 1998 and 1999. Data plots represent 3-day moving averages and the trend lines are linear. Positive Del T represents stable atmospheric conditions and negative Del T represents unstable conditions.

increase from negative around the summer solstice to large positive before final freeze up. For the total measurement period of 1999 (Fig. 8), which represents most of the open-water season, Q_{ST} gives a net of 204 MJ m^{-2} (Table 5). This represents 19% of the total heat storage that would be lost in the remainder of the open-water season and during the ice-covered winter period if an annual balance is achieved. Most of the radiant energy used to heat the lake during the summer is utilized in strong sensible and latent heat fluxes in late summer, fall, and early winter. This is evident in Table 5 where, during the stable atmosphere period (SAP), Q^* is 6 times larger than during the unstable atmosphere period (UAP), and the total sensible and latent heat fluxes, $Q_E + Q_H$, are 9 times larger during UAP than during SAP. The spikes in Q_E and Q_H (Fig. 8) are due to strong wind activity, that deeply mixes the lake waters and enhances turbulent exchange, a theme introduced by Blanken et al. (2000) and explored in detail by Blanken et al. (2003). For Q_E during 1999, these strong sensible and latent heat releases are equally as prominent in the SAP and UAP periods (Fig. 8). The patterns and magnitude of Q_{ST} follow closely calorimetric storage calculations for the whole lake as shown in Schertzer et al. (2003).

f. Evaporation

Cumulative evaporation (Fig. 9) adds 1999 data to the results published by Blanken et al. (2000). As noted in that study, the El Niño year of 1998 had greatly enhanced evaporation totals compared to 1997, and approached average values for the lower Laurentian Great Lakes (Schertzer and Croley 1999). Total E for 1999 lies midway between those 2 yr (Table 6). Figure 10 clearly indicates the increase in evaporation rates as the season progresses. The trend lines indicate that in 1997 and 1998 the rate accelerated as the season progressed

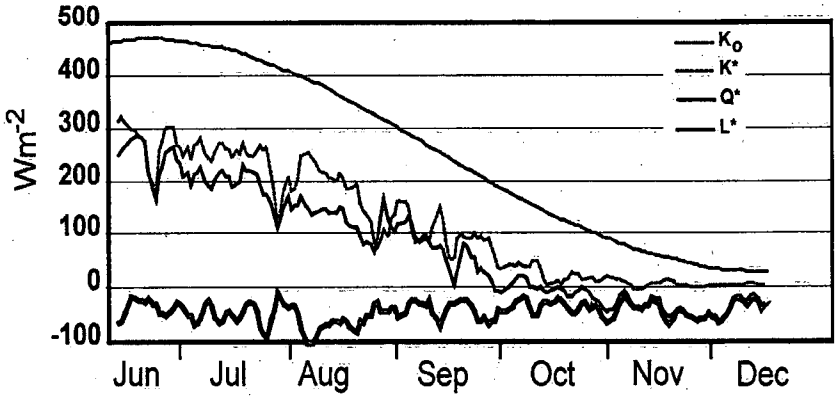

FIG. 6. Three-day moving averages of radiation fluxes during the 3 yr of measurement; K_0 is extraterrestrial solar radiation, K^* is net solar radiation, Q^* is net all-wave radiation, and L^* is net longwave radiation.

TABLE 4. Radiation values for an 11-day common period (27 Jul–6 Aug) for the 3 yr of measurement; K_0 is extraterrestrial solar radiation, K^* is net solar radiation, Q^* is net all-wave radiation, and L^* is net longwave radiation. Flux values are in W m^{-2}.

	K_0	K^*	Q^*	L^*	K^*/K_0	Q^*/K_0
1997	406	207	129	−78	0.51	0.32
1998	406	195	143	−52	0.48	0.35
1999	406	195	147	−48	0.48	0.36

right through to final freeze up, whereas in 1999, it decelerated slightly toward the end of the open-water season. From 85% to 90% of total evaporation occurs after mid-August during the UAP (Table 6).

4. Discussion

The results from this paper present a clear picture of the seasonal thermal and energy regimes at the water–air interface in the central portion of this large northern lake. In many respects it is a similar picture to that for the Laurentian Great Lakes as documented by Schertzer (1997). However, the high-latitude position exerts some singular characteristics on the seasonality, such as the apparent disconnect between the surface radiation balance and the sensible and latent heat fluxes. This is the most striking anomaly with the normal behavior of a terrestrial surface and, in this respect, the lake behaves more like higher-latitude oceans. After final ice melt, which coincides more or less with the summer solstice, the radiation balance becomes strongly positive (Fig. 6), due to the small surface albedo that averages 6% at that time of year (Blanken et al. 2000). The lake down to a depth of 10 m strongly absorbs solar radiation, as is evident in Table 2. Because of the stable atmosphere, Q_E and Q_H are small. Thus, the net solar radiation is largely used in heating the lake, a situation that persists until mid- to late August (Fig. 4). Subsequently, the absorbed solar radiation is small (Fig. 6), and with the change over to an unstable atmosphere, the sensible and latent heat fluxes become the dominant agents of energy exchange. These grow in magnitude into the winter, as the atmospheric instability increases, and stronger winter winds result in increased lake mixing that exposes the warm water to the cold atmosphere. The net heat storage is strongly seasonal with very large storage during the stable atmospheric period and large loss during the unstable atmospheric period. These processes and patterns are all interrelated. The lake must warm until the surface temperatures exceed atmospheric temperatures to create an unstable atmosphere, and there can only be a sensible heat loss when the atmosphere is unstable. The latter is not true of the evaporative heat loss, however, because lapse vapor pressure gradients can occur under inversion conditions. However, they are less common than in an unstable atmosphere.

The evaporation regime is especially important to the hydrometeorology of the lake, its region, and to some extent the lower Mackenzie River basin. Between early 1998 and 2001 the water level in Great Slave Lake fell by about 1 m, as indicated by water level records near Yellowknife and confirmed by water markings on the rocks of the Inner Whaleback Islands. Much of this decrease can be attributed to the enhanced evaporation in this warm period, especially during the El Niño year, as well as to similar enhanced evaporation from lakes in the GSL catchment area and upstream (especially Lake Athabasca). Lower lake levels affect the hydraulic head to the downstream portions of the river system and, hence, streamflow rates. Such major reservoirs exert time lags into the flow system that can be significant on interannual timescales.

The single most important factor, to the seasonal energy balance and to interannual variability, is the date of final ice breakup. An especially early breakup due to higher than normal temperatures, as in 1998, takes advantage of the strong solar insolation in the high-sun season of early June, and gives an early start to the heating of the lake. The lake reaches its maximum temperature and heat storage earlier (Schertzer et al. 2002a), and changes from a stable to an unstable atmospheric

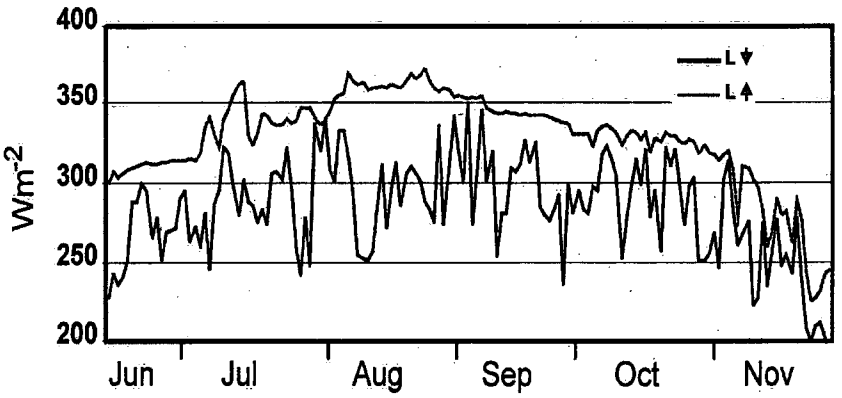

FIG. 7. Incoming (L↓) and outgoing (L↑) longwave radiation fluxes in 1999. Values represent 3-day moving averages.

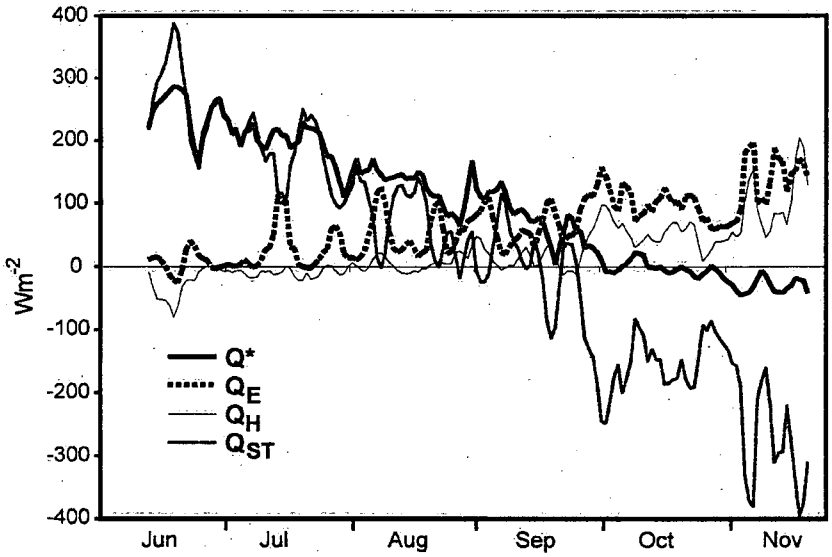

FIG. 8. The energy balance at Inner Whaleback Island in 1999; Q^*, Q_E, Q_H, and Q_{ST} designate net radiation, latent heat flux, sensible heat flux, and calculated change in storage, respectively.

regime sooner. This promotes the sensible and latent heat fluxes. If coincidentally, the fall and early winter is warmer than normal it helps to delay final freeze, as in 1998, and this prolongs the period of maximum sensible and latent heat fluxes. Thus, in 1998, the total evaporation exceeded that of the other two warmer-than-normal years by an average 25% and all of this difference occurred after mid-August. Although the results of this study cannot support it, a reasonable hypothesis is that later spring thaw will have the converse effect. In that scenario, the lake cannot absorb large insolation in spring, and the resulting heat storage before the lake begins to cool is of lesser magnitude. This heat will be released during the unstable atmosphere period, but of necessity this period will be shorter or, alternatively, the sensible and latent heat fluxes to the atmosphere will be of lesser magnitude. Either way the result is less direct heating of the atmosphere and less evaporation.

Large northern lakes are very dynamic systems that can undergo large interannual variability that has potentially significant impact on the regional hydrometeorology and hydrology. They comprise a substantial component of the total surface area in many parts of the high latitudes. Numerical models of the thermal regime of these large lakes need to be developed and interfaced with regional climate models (MacKay et al. 1998; Schertzer and Croley 1999; Schertzer and Lam 2000; Schertzer et al. 2000b).

5. Conclusions

The general seasonal patterns found in this study are believed to represent the midlake regimes of other large northern lakes in the Canadian Shield. Atmospheric and lake thermal regimes interact closely. Temperature differences between midlake and the northern shore follow a seasonal linear change from close to 6°C colder midlake in June, to 6°C warmer in December. These differences are a response to the seasonality in the surface energy budget of the lake. The surface radiation balance and the sensible and latent heat fluxes are not related on a day-to-day basis. From final lake ice melt in mid-June, through to mid- to late August, the top 10 m of the lake is able to absorb more than one-half of the extraterrestrial solar radiation. Under a stable atmosphere during this period, the sensible and latent heat fluxes are small and the net solar radiation is largely used in heating the lake. After mid-August through to final freeze in mid-December to early January, the at-

TABLE 5. Net radiation, Q^*; latent heat flux, Q_E; sensible heat flux Q_H; and calculated change in storage, Q_{ST}, for the season (TOTAL) for 1999 and for SAP from 12 June to 22 August and the UAP from 23 Aug to 18 Nov as shown in Fig. 8. All values are in MJ m^{-2}.

	Q^*	Q_E	Q_H	Q_{ST}
TOTAL	1390	887	299	204
SAP	1192	182	−67	1076
UAP	198	705	366	−872

TABLE 6. Total evaporation (mm) for the open-water season (TOTAL) and for the SAP and UAP for each year.

	TOTAL	SAP	SAP/TOT	UAP	UAP/TOT
1997	384	54	0.15	325	0.85
1998	506	51	0.10	455	0.90
1999	417	62	0.15	356	0.85
Avg	436	56	0.13	379	0.87

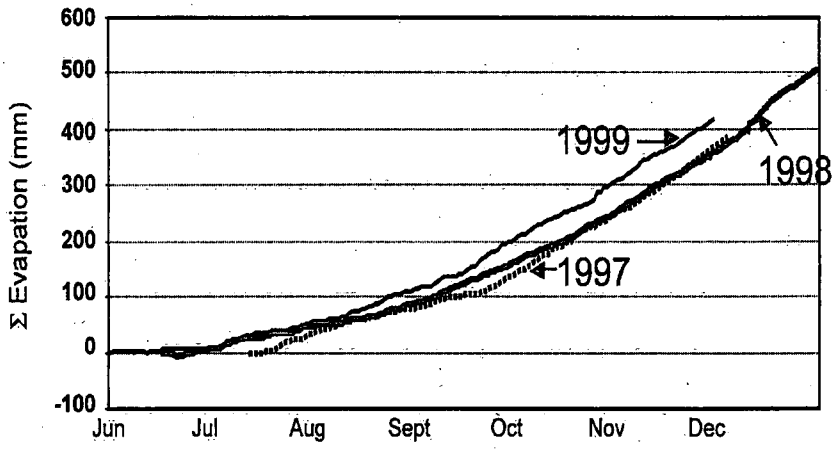

FIG. 9. Cumulative evaporation, ΣEvaporation, during the 3 yr of measurement.

mosphere becomes increasingly unstable. The absorbed solar radiation is small and the sensible and latent heat fluxes become the dominant agents of heat exchange and grow in magnitude into the winter season. In 1999, comparing the periods of stable and unstable lower atmospheric conditions, net radiation is 6 times larger during the stable atmospheric regime and, conversely, the combined sensible and latent heat fluxes are 9 times larger during the unstable atmospheric regime. From 85% to 90% of total evaporation occurs after mid-August, and evaporation rates increase continuously through to final freeze up, though the rates of increase vary from year to year.

The date of final ice melt in June exerts the largest single control on the seasonal thermal and energy regimes of these large northern lakes. An early thaw greatly enhances the magnitude of absorbed solar radiation in the high-sun season. This becomes stored heat energy that drives the large sensible and latent heat fluxes during fall and early winter. A late thaw will have the opposite effect and will result in smaller late-season fluxes and/or an earlier final freeze up.

Acknowledgments. Financial support for this project was provided by network research grants from the Meteorological Service of Canada (MSC) and the Natural Science and Engineering Research Council of Canada (NSERC) to the Mackenzie GEWEX Study, individual NSERC research grants, a research grant from NASA, and student northern training grants from the Canada Department of Indian and Northern Affairs. Logistical and equipment support during measurement campaigns has been provided by the Great Slave Lake branch of the Canadian Coast Guard, Environment Canada, Institute of Hydrology, MSC, National Water Research Institute, Royal Canadian Mounted Police Marine Unit, and Water Survey of Canada. Lake thaw and freeze-up data have been provided by Ann Walker, MSC. Bob Kochtubajda, Environment Canada, provided meteoro-

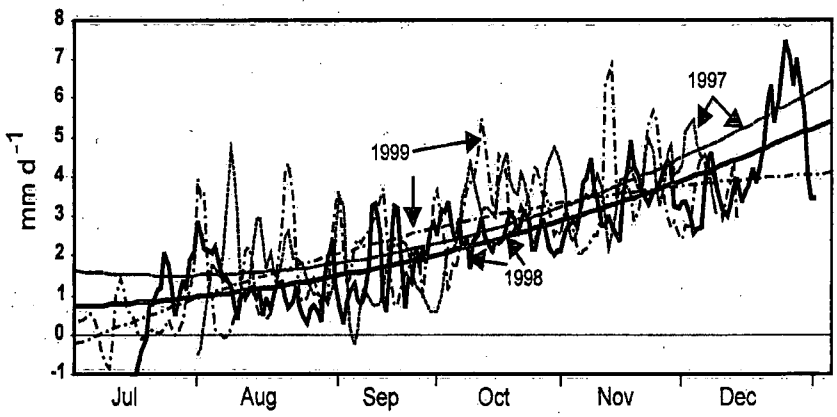

FIG. 10. Evaporation rates during the 3 yr of measurement. The data plotted are 3-day moving averages and the trend lines are second-order polynomials.

logical data, and Cliff Brettle designed and constructed instrument mounts and enclosures.

REFERENCES

Blanken, P. D., and Coauthors, 2000: Eddy covariance measurements of evaporation from Great Slave Lake, Northwest Territories, Canada. *Water Resour. Res.*, **36,** 1069–1078.

——, W. R. Rouse, and W. M. Schertzer, 2003: Enhancement of evaporation from a large northern lake by the entrainment of warm, dry air. *J. Hydrometeor.*, **4,** 680–693.

Harbeck, G. E., 1962: A practical field technique for measuring reservoir evaporation utilizing mass-transfer theory. U.S. Geological Survey Professional Paper 272-E, 101–105.

MacKay, M. D., R. E. Stewart, and G. Bergeron, 1998: Downscaling the hydrological cycle in the Mackenzie Basin with the Canadian Regional Climate Model. *Atmos.–Ocean,* **36,** 179–211.

Quinn, F. H., 1978: An improved aerodynamic evaporation technique for large lakes with application to the IFYGL. *Water Resour. Res.,* **15,** 935–940.

——, and G. den Hartog, 1981: Evaporation synthesis. *IFYGL—The International Field Year for the Great Lakes,* E. J. Aubert and T. L. Richards, Eds., NOAA Great Lakes Environmental Research Laboratory, 221–245.

Rawson, D. S., 1950: The physical limnology of Great Slave Lake. *J. Fish. Res. Board Can.,* **8,** 3–66.

Rouse, W. R., P. D. Blanken, A. K. Eaton, and R. M. Petrone, 1999: Evaporation from wetlands and large lakes. *Proc. Fourth Scientific Workshop for the Mackenzie GEWEX Study (MAGS),* Montreal, QC, Canada, NSERC and AES, Environment Canada, 32–35.

——, ——, W. M. Schertzer, and C. Spence, 2000: The role of lakes in the surface climates of cold regions. *Proc. GAME-MAGS Int. Workshop,* Nagoya, Japan, Institute for Hydrospheric–Atmospheric Science, Nagoya University, Research Rep. 7, 77–80.

——, C. M. Oswald, C. Spence, W. R. Schertzer, and P. D. Blanken, 2002: Cold region lakes and landscape evaporation. *Proc. Second MAGS-GAME Int. Workshop,* Sapporo, Japan, Institute for Low Temperature Science, University of Hokkaido, 37–42.

——, and Coauthors, 2003: Energy and water cycles in a high latitude, north-flowing river system: Summary of results from the Mackenzie GEWEX Study—Phase 1. *Bull. Amer. Meteor. Soc.,* **84,** 73–87.

Schertzer, W. M., 1997: Freshwater lakes. *The Surface Climates of Canada,* W. G. Bailey, T. Oke, and W. R. Rouse, Eds., McGill-Queens University Press, 124–148.

——, and T. E. Croley II, 1999: Climate and lake responses. *Potential Climate Change Effects on Great Lakes Hydrodynamics and Water Quality,* D. C. L. Lam and W. M. Schertzer, Eds., American Society of Civil Engineers, 1–74.

——, and D. C. L. Lam, 2000: Modeling of climate-change on large lakes and basins with consideration of effects in related sectors. Contributions to the International Hydrological Programme (IHP-V) by Canadian Experts, UNESCO IHP Tech. Doc. in Hydrology 33, 127–155.

——, W. R. Rouse, and P. D. Blanken, 1999: Cross-lake variation of evaporation, radiation and limnological processes in Great Slave Lake. *Proc. Fourth Scientific Workshop for the Mackenzie GEWEX Study (MAGS),* Montreal, QC, Canada, NSERC and AES, Environment Canada, 36–42.

——, ——, and ——, 2000a: Cross-lake variation of physical limnological and climatological processes of Great Slave Lake. *Phys. Geogr.,* **21,** 385–406.

——, ——, and ——, 2000b: Modelling of large lakes in cold regions. *Proc. GAME-MAGS Int. Workshop,* Nagoya, Japan, Institute for Hydrospheric–Atmospheric Science, Nagoya University, Research Rep. 7, 126–129.

——, ——, A. E. Walker, N. Bussières, H. G. Leighton, and P. D. Blanken, 2002: Heat exchange, evaporation and thermal responses of high latitude lakes. *Proc. Second MAGS-GAME Int. Workshop,* Sapporo, Japan, Institute for Low Temperature Science, University of Hokkaido, 43–51.

——, ——, P. D. Blanken, and A. E. Walker, 2003. Over-lake meteorology and estimate bulk heat exchange of Great Slave Lake in 1998 and 1999. *J. Hydrometeor.,* **4,** 649–659.

Shuttleworth, W. J., J. H. C. Gash, C. R. Lloyd, D. D. McNeil, C. J. Moore, and J. S. Wallace, 1988: An integrated micrometeorological system for evaporation measurement. *Agric. For. Meteor.,* **43,** 295–317.

Stewart, R. E., and Coauthors, 1998: The Mackenzie GEWEX Study: The water and energy cycles of a major North American river system. *Bull. Amer. Meteor. Soc.,* **79,** 2665–2683.

Walker, A., A. Silis, J. Metcalf, M. Davey, R. Brown, and B. Goodison, 1999: Snow cover and lake ice determination in the MAGS region using passive microwave satellite and conventional data. *Proc. Fourth Scientific Workshop for the Mackenzie GEWEX Study (MAGS),* Montreal, QC, Canada, NSERC and AES, Environment Canada, 89–91.

PRINTED IN CANADA
IMPRIMÉ AU CANADA
ON RECYCLED PAPER
SUR DU PAPIER RECYCLÉ

National Water Research Institute
Environment Canada
Canada Centre for Inland Waters
P.O. Box 5050
867 Lakeshore Road
Burlington, Ontario
L7R 4A6 Canada

National Hydrology Research Centre
11 Innovation Boulevard
Saskatoon, Saskatchewan
S7N 3H5 Canada

NATIONAL WATER RESEARCH INSTITUTE
INSTITUT NATIONAL DE RECHERCHE SUR LES EAUX

Institut national de recherche sur les eaux
Environnement Canada
Centre canadien des eaux intérieures
Case postale 5050
867, chemin Lakeshore
Burlington, Ontario
L7R 4A6 Canada

Centre national de recherche en hydrologie
11, boul. Innovation
Saskatoon, Saskatchewan
S7N 3H5 Canada

Environment Canada Environnement Canada

Canada